



EXPERIMENTAL INVESTIGATION OF WIND PRESSURE FIELDS ON BUILDINGS WITH GABLED ROOFS HAVING DIFFERENT PITCH ANGLES

Yücel ÖZMEN* and Ertan BAYDAR**

*Department of Mechanical Engineering Karadeniz Technical University
61080 Trabzon, yozmen@ktu.edu.tr

**Department of Mechanical Engineering Karadeniz Technical University
61080 Trabzon, baydar@ktu.edu.tr

(Geliş Tarihi: 21.12.2015, Kabul Tarihi: 24.03.2016)

Abstract: A wind tunnel study was carried out to investigate wind pressure distributions on the three gables roofed building models of 15°, 30°, and 45° roof pitch and determine the effect of roof pitch on the external wind pressure. The surface pressure measurements were performed on the roofs and side walls of the building models facing a turbulent wind of 15 m/s and the values of mean and peak pressure coefficients were obtained for wind angles from 0° to 360° with 15° increment. The pressure distributions on the roofs are significantly influenced by the roof pitch. The roof pitch of 15° produces more critical suction on the roof than those of 30° and 45° roof pitches. The highest peak suction is experienced with 15° pitched roof at the windward roof corner for the wind angle of 15°. Pressure contour distributions on the building models show that wind angle of 45° is more critical than wind angles of 0° and 90°.

Keywords: Wind tunnel, Low-rise building, Gable roof, Roof pitch, Pressure coefficient, Suction

FARKLI EĞİM AÇILARINA SAHİP BEŞİK ÇATILI BİNALAR ÜZERİNDE RÜZGAR BASINÇ ALANLARININ DENEYSEL İNCELENMESİ

Özet: Bu çalışmada, rüzgar tüneli test bölgesine yerleştirilmiş 15°, 30° ve 45° çatı eğimlerine sahip beşik çatılı bina modelleri üzerinde rüzgar basınç dağılımları incelenmiş ve çatı eğiminin basınç dağılımları üzerindeki etkisi belirlenmiştir. 15 m/s'lik serbest akış hızına maruz bina modellerinin yan duvarları ve çatıları üzerinde yüzey basınç ölçümleri gerçekleştirilerek, 0° ile 360° arasındaki rüzgar geliş açılarında 15°'lik aralıklarla ortalama ve pik basınç katsayıları elde edilmiştir. Basınç dağılımları çatı eğiminden önemli oranda etkilenmektedir. 15° eğimli çatı durumunda çatı üzerindeki emme etkileri 30° ve 45° eğimli çatılara göre daha kritik olmaktadır. En kritik emme etkisi, 15° çatı eğimine sahip bina modelinin rüzgar tarafındaki çatı köşesi yakınında 15°'lik rüzgar geliş açısında oluşmaktadır. Model yüzeylerinde eş basınç alanları şeklindeki dağılımlar, emme etkisi açısından 45°'lik rüzgar geliş açısının 0° ve 90°'lik rüzgar geliş açılarına göre daha kritik olduğunu göstermektedir.

Anahtar Kelimeler: Rüzgar tüneli, Alçak bina, Beşik çatı, Çatı eğimi, Basınç katsayısı, Emme

NOMENCLATURE

C_p	Pressure coefficient [$\Delta P / (\rho U_o^2/2)$]
C_{pmean}	Mean pressure coefficient
C_{prms}	RMS pressure coefficient
C_{pmax}	Maximum pressure coefficient
C_{pmin}	Minimum pressure coefficient
H	Model height [m]
L	Model length [m]
ΔP	Difference between the surface pressure and the atmospheric pressure [N/m^2]
P	Pressure [N/m^2]
P_o	Atmospheric pressure [N/m^2]
Re	Reynolds number [$U_o H/\nu$]
U_o	Free stream velocity [m/s]
u	Velocity components in x direction [m/s]
$\sqrt{u^2}$	Turbulent velocity in x direction [m/s]
v	Velocity components in y direction [m/s]
W	Model width [m]

x	Horizontal coordinate
y	Vertical coordinate
δ	Boundary layer thickness [m]
α	Roof slope [$^\circ$]
θ	Wind angle [$^\circ$]
ν	Kinematic viscosity [m^2/s]
ρ	Density of air [kg/m^3]
n	Power

INTRODUCTION

Wind is one of the significant forces of nature that must be considered in the design of a building. Wind pressures acting on buildings are highly fluctuating since they are located in the lower part of atmospheric boundary layer where wind turbulence and gradient of wind speed dominate. The loading effects of the natural wind on buildings are rather complicated interactive process between the wind flow and the various components of the building.

The majority of structures built all over the world can be categorized as low-rise buildings used for residential, commercial and other purposes. These buildings are generally exposed to wind damage caused by typhoons, hurricanes, etc. Damage to the buildings results from aerodynamic wind pressure that develop as air flow over and around the building. Depending on the past damage investigation reports, most of the wind damage was on the envelope of buildings, in particular at the roof sheathing (Kumar and Stathopoulos (1998)). These evidences indicate that an improvement in wind resistance of the building's envelope would result with a significant reduction in overall economic losses. For these purposes, a detailed understanding about the wind effects on low-rise buildings, and in particular, on roof sheathing is necessary.

The characteristics of wind pressure fluctuations depend on numerous factors such as mean wind speed and direction, terrain condition, surroundings, structural geometry, surface texture etc. Despite a number of studies made in the past, there are many problems such as mechanism of peak suction and conical vortices on roofs remaining unsolved. Recently, significant improvements in experimental techniques have been made and these new techniques enable us to understand the structure of the pressure fields on the buildings extensively. Wind tunnel studies on the wind loading of low-rise building roofs began in the mid-1960s and accompanied with researches on new techniques for accurate wind tunnel simulation. Several fundamental experiments carried out with three-dimensional bluff bodies to understand the flow around these bodies. Studies on flows fields over the building roofs focused on pressure measurements. Davenport and Surry (1974) investigated the pressure distributions over the roofs of low-rise buildings. The results showed that the mean and peak pressure coefficients were much greater for smooth terrains than for rough or build-up terrains and oblique winds produced more critical pressures on the roof than normal and parallel winds. Stathopoulos (1984) examined mean and root-mean-square (rms) pressures for 0°, 22.5° and 45° roof pitches. They observed that high suction appear on the edges and corners of flat roofs, decrease on 22.5° roof and disappear on 45° roof.

Holmes (1981) conducted some experiments with a set of gable buildings with overhangs for roof pitches of 10°, 15°, 20° and 30°. He indicated that the turbulence characteristics in the flow have strong influence on the roof wind loads. Stathopoulos and Mohammadian (1986) experimentally determined the wind pressure loads for mono-sloped roof buildings by testing a variety of models exposed to a simulated atmospheric boundary layer flow over an open country terrain. Experimental data indicated that both the mean and the instantaneous peak wind pressures are higher than those found previously for buildings with gabled roofs. Saathoff and Melbourne (1989) studied the peak roof loading generation mechanism by investigating the large pressure formations and the accompanying vortex generation. He observed the intermittent peaks when the separated wind flow rolled up to form a large vortex near the surface. Meecham *et al.* (1991) derived aerodynamic data for 4:12 hip and gable roofs. They observed that in severe wind storms, hip roofs seem to survive much better than

gable roofs. Agui and Andreopoulos (1992) conclude from the pressure fluctuation measurements that the large scale structures play an important role in the dynamics of separated flow. Ginger and Letchford (1992) investigated the flow separation and vortex formation mechanism on a set of canopy roofs with the roof pitches of 0°, 5°, 10°, 15°, 22.5° and 30°. They reported that the peak loads on roof corners are accompanied by a stable conical vortex for the whole set of the slopes tested under the oblique wind attacks. Kanda and Maruta (1993) experimentally investigated the characteristics of mean and peak wind pressures on the long low-rise buildings with gable roof. They found that the large negative values of mean and peak wind pressures are generated on the leeward surface for the wind direction of 45°. Barnard and Driviere (1994) investigated the wind velocity and pressure fields over the roof of a model of Aylesbury experimental house. They noted that there is no consistent correlation between velocity and pressure fields. Ginger and Letchford (1995) conducted point and area-averaged pressure measurements on a 1:100 scaled building roof immersed in a simulated suburban atmospheric surface layer in wind tunnel. They noted that large magnitude mean and fluctuating pressures were measured within regions of flow separation on low rise building roofs. Kawai and Nishimura (1996) noted that the most critical suction loads occur near the roof corner of windward side for inclined wind directions because of conical vortex on a flat roof model for uniform and turbulent flow conditions. Kumar and Stathopoulos (1998) measured the power spectra of wind-induced pressures at various tap locations on the roofs of several low building models placed in two different terrains. They determined the characteristic shape of building models and derived a suitable analytical model for their representation. The results showed that spectra vary under different conditions and a well normalized spectra is identical in many situations. Case and Isyumov (1998) presented comparisons of local pressures and selected structural loads experienced by the low buildings in the suburban and open country exposures. They showed that the suburban exposure produces lower wind loads than those experienced in the open country exposure. Ginger *et al.* (2000) conducted a series of measurements for distribution of mean and peak pressure on a typical low-rise building roof with 1:50 scaled wind tunnel study. The most critical wind loads occur near the roof edge of windward side. Banks *et al.* (2000) showed that the largest mean and peak suction values on the roof of a low rise building are observed on taps beneath the conical delta-wing type corner vortices that occur for oblique winds. Ginger and Holmes (2003) studied on long, low-rise buildings with a steep roof pitch, to determine the effect of the length-to-span aspect ratio on the external wind pressure distributions. They found a significant increase in the magnitude of the negative pressure coefficients on the leeward roof and wall, with an increase in aspect ratio for oblique approach winds. Guirguisa *et al.* (2007) examined the characteristics of wind flow that pass from simplified models of one-side pitched roof buildings in a wind tunnel. They found that pitch angle affect the mean static pressure on the roof. Prasad *et al.* (2009) carried out wind tunnel testing of low-rise building models with flat, gabled and hip roof configurations in a boundary layer wind tunnel. For the gabled and the hip

roofs, the 15°, 20°, 30° and 45° pitch angles were investigated. They found that the suction over the roof is significantly influenced by the roof configuration. For the hip roof, the peak suction is reduced by 42% compared to the gabled roof. John *et al.* (2011) studied on the wind loads of gable roof building with interference of boundary wall in wind tunnel. They observed that the pressure values reduce significantly due to the presence of boundary wall. Hu *et al.* (2011) conducted an experimental study to quantify the characteristics of a tornado-like vortex and to reveal the dynamics of the flow-structure interactions between a low-rise, gable-roof building model and swirling, turbulent tornado-like winds. Gavanski *et al.* (2013) examined wind loads acting on roof sheathing on typical low-rise, wood-frame houses for a variety of parameters including roof shape, roof pitch, building height, upstream terrain and the presence of surrounding structures placed in several patterns. They noted that roof shape and upstream terrain have the most significant effect on wind loads acting on roof sheathing. The microburst wind loading effects on a set of low-rise building models have been investigated by Zhang *et al.* (2014). They observed that at or near the center of the microburst, high external pressures occur for all structures, resulting in a large downward force on the roof.

The dynamic loads forming on the buildings and on their roofs due to changing atmospheric conditions cause negative effects such as collapse of buildings or movement of roofs. According to wind damage reports, low-rise buildings with gable roofs are more exposed to these kinds of negative effects (Kumar (1997)). Hence, pressure distributions on the gable roofs must be considered to evaluate these negative effects of wind. Although extensive researches are conducted on the aerodynamics of low-rise buildings, most of the studies cover a narrow aspect. This study aims to find out most of the building roof parameters systematically. There is a lack of research on the effect of roof pitches considering all factors extensively. The purpose of this study is to investigate the distributions of wind loads on the gable roofed building models, to reveal the changes in pressure distributions and to help to better understand the changing mechanism of pressure fields. For this reason, three gable roofed building models of 15°, 30°, and 45° roof pitches are introduced to examine their influence on the pressure distributions.

EXPERIMENTAL STUDY

The experiments carried out in a low speed, open circuit wind tunnel at the Karadeniz Technical University. The wind tunnel has a working section of 457 mm wide, 457 mm high and 2450 mm long. The combination of barrier, vortex generators and roughness elements at the entrance to the test section is used to simulate atmospheric boundary layer (power-law exponent, $n=0.2$) over a city suburb. Models are constructed to a geometric scale of 1:100. A turbulent boundary layer of 150 mm thickness is obtained at the free stream velocity of 15 m/s, giving a Reynolds number based on building height of $Re=52000$. Figure 1 indicates a schematic diagram of the wind tunnel test-section and the measurement system. δ and H represent the boundary layer thickness and characteristic height of models, respectively.

The ratio of boundary layer thickness to model height (δ/H) is 2.9. The mean and fluctuating surface pressure measurements are conducted with a measurement chain system consisting of the components of signal conditional module, Setra 239 pressure transducer, A/D converter, package and computer. The output of the pressure transducer is fed through a signal conditioning unit before being digitized and recorded. The signals from the transducer are sampled at a rate of 1000 samples per second for a period of 16 s and data are low-pass filtered at 300 Hz. The mean and fluctuating velocity measurements at the reference boundary layer are performed with TSI IFA 100 constant-temperature anemometer and TSI model 1211 hot-film probe.

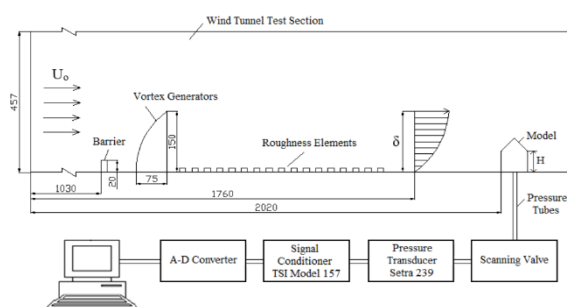


Fig 1. Wind tunnel test section and pressure measurement system

The dimensions of gabled roof models with the distribution of measurement taps on their surfaces are shown in Figure 2. The models with gable roofs of 15°, 30°, and 45° roof pitches (α) made of plexiglas have $H=52$ mm height, $W=65$ mm width and $L=130$ mm length. The aspect ratio (wall length to wall width) of the building models is chosen as 2:1. Pressure taps are intensified on the critical parts of the models. The models are placed at a distance of $4H$ from the reference boundary layer. As stated by Oliveira and Younis (2000), this distance must be at least $3H$ because reference boundary layer must not be affected from the existence of model. To measure pressure distributions on the models, pressure taps of 15 mm long pieces with 1.6 mm external diameter and 1 mm internal diameter stainless-steel tubing are inserted into the holes drilled in the plexiglas. The numbers of pressure taps on the building models are 101, 101 and 124 for the 15°, 30°, and 45° roof pitches, respectively. The models are rotated from 0° to 360° wind angle (θ) with 15° increment in clockwise direction to facilitate measurements over the entire roofs and side walls. Symmetry is used to reduce the number of measurements. A scanning valve with 48 ports is used to supply a link from pressure taps to the pressure transducer. All pressure taps are connected to the scanning valve using the vinyl tubing of 60 cm lengths and 1 mm inside diameter. A conventional restricted tube system (0.3 mm internal diameter) with a flat frequency response up to the 100 Hz is used as the transfer medium between the tap and the Setra 239 transducer. The blockage ratio for the models in the wind tunnel ranged from 3.7 to 5.2 %. Correction for the effect of the wind tunnel blockage is also done.

The uncertainties in the measurements of the axial mean velocity and axial turbulence velocity are estimated to be

less than $\pm 2.07\%$ and $\pm 4\%$, respectively. Mean and fluctuating pressures have a corresponding estimated uncertainty of $\pm 3.06\%$ and $\pm 4.6\%$, respectively Holman (1994). The experimental results are reproducible within these uncertainty ranges.

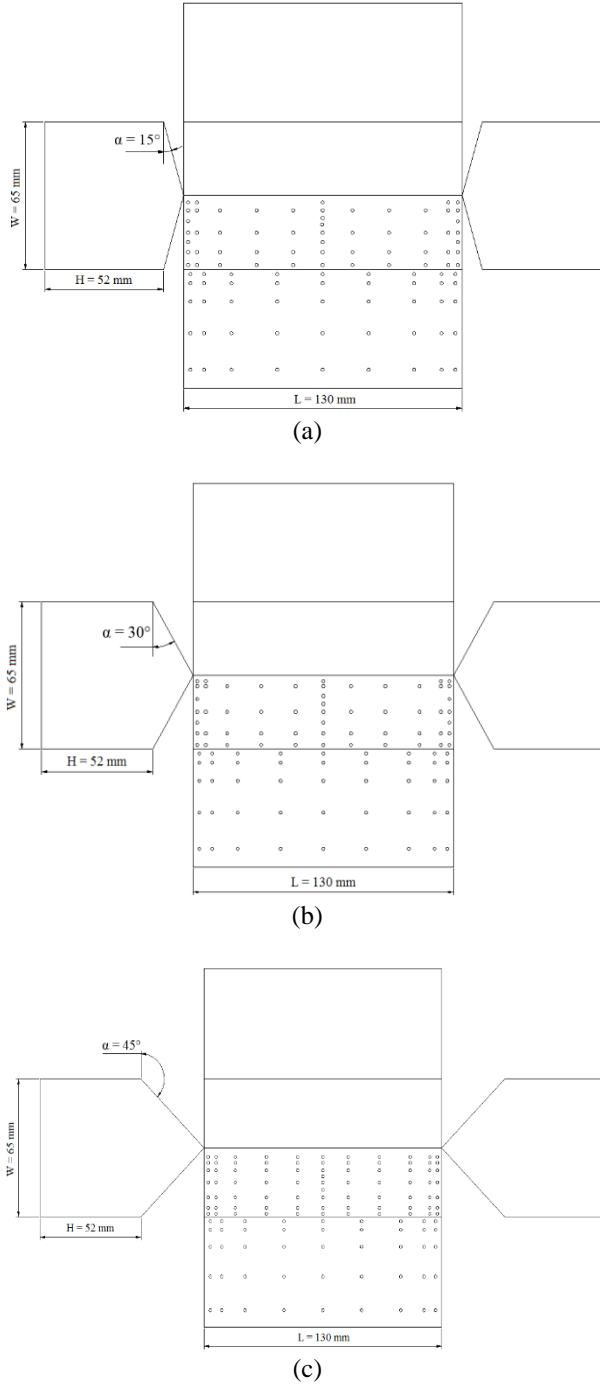


Figure 2. Dimensions of gabled roof building models and the locations of pressure taps (a) $\alpha=15^\circ$ (b) $\alpha=30^\circ$ (c) $\alpha=45^\circ$

RESULTS AND DISCUSSION

The mean velocity and turbulence intensity profiles of the streamwise velocity component measured at the reference boundary layer are shown in Figure 3. It is seen that the mean velocity profile in the reference boundary layer agrees well with the power law of $n=0.2$ and the turbulence intensity near the wall reaches up to 11%.

The resulting data consists of mean, maximum, minimum and root-mean-square (rms) values of the surface pressure which are normalized by the free stream mean dynamic pressure ($0.5\rho U^2$). The definition of the coefficients is shown below with positive external pressure acting towards the surface and suction away.

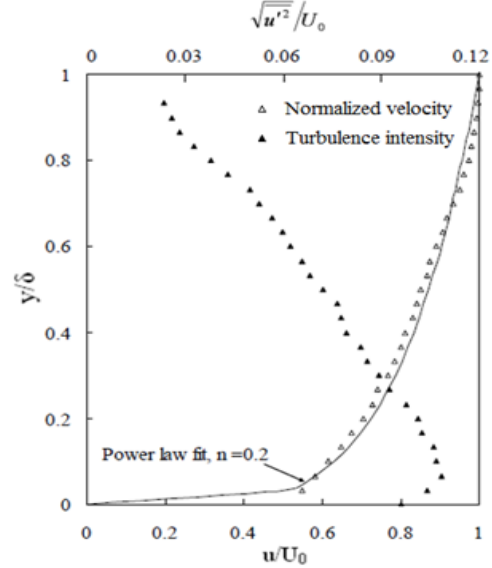


Figure 3. Profiles of mean velocity and turbulence intensity

Mean pressure coefficient,

$$C_{p\text{mean}} = \frac{\bar{P} - P_s}{\rho U^2 / 2} \quad (1)$$

Root mean square (Rms) pressure coefficient,

$$C_{p\text{rms}} = \frac{\tilde{P} - P_s}{\rho U^2 / 2} \quad (2)$$

Maximum peak pressure coefficient,

$$C_{p\text{max}} = \frac{\hat{P} - P_s}{\rho U^2 / 2} \quad (3)$$

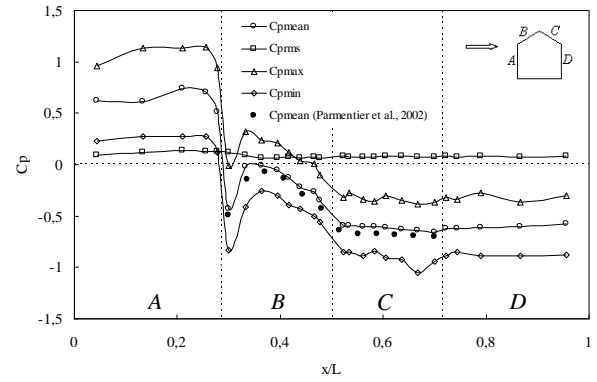
Minimum peak pressure coefficient,

$$C_{p\text{min}} = \frac{\check{P} - P_s}{\rho U^2 / 2} \quad (4)$$

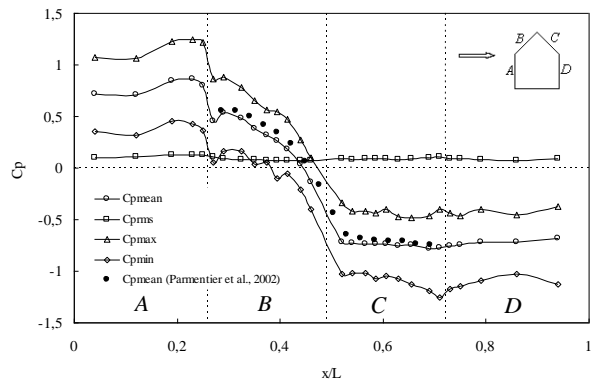
In these equations; \bar{P} is local mean surface pressure, \tilde{P} is root mean square (rms) surface pressure, \hat{P} is maximum peak pressure, \check{P} is minimum pressure and P_s is atmospheric pressure. The variations of mean, rms, maximum and minimum values of pressure coefficients along the mid-axes of three gabled roofed building models for $\theta=90^\circ$ wind angle are given comparatively with the measurements of Easom (2000) and Parmentier *et al.* (2002) in Figures 4a-c for the 15° , 30° , and 45° roof pitches respectively. Pressure distributions on the windward walls of building models are positive due to pushing effect. Negative pressure fields occur both on the roofs and leeward walls of the building models due to flow separating from the leading edges and ridges of the roofs. For the 15° roof pitch, the flow separating from the leading edge of the model reattaches on the windward surface of the roof and then re-separates from the roof ridge. The

largest negative pressure occurs in separation flow region near the leading edge of the roof and reduces in magnitude progressively in the reattachment region on the roof surface. Pressure distribution along the leeward wall is almost uniform and below the atmospheric pressure (Figure 4a). Negative pressure distributions on the leeward roof and rear wall have the same magnitudes and they are stronger than the negative pressures on the windward roof except leading edge region in case of 30° roof pitch (Figure 4b). For the 45° roof pitch, pressure distributions are positive on the windward wall and on the large part of the windward roof which is directly exposed to the wind. Due to the flow separation from the roof ridge, negative pressure distributions occur on the leeward roof and wall with the same magnitudes (Figure 4c). It is clear from Figures 4a-c that there are good accordance between the measured mean pressure distributions of present study and Easom (2002) and Parmentier *et al.* (2002) measurements for all three roof pitches.

Figures 5a-c show the variations of the mean, rms, maximum and minimum pressure coefficients at the critical tap 1 positioned near the windward roof corner with wind angle of attack for the 15°, 30°, and 45° gable pitched roofs respectively. The critical wind directions in which the largest peak suction occurs can be identified at the tap 1 for the windward roof corner. It is seen that the critical wind angle is 15° for all tested roof pitches. The most critical minimum pressure coefficients at this wind angle are -3.36, -2.31 and -1.95 for the 15°, 30°, and 45° roof pitches respectively. Figures 6a-c give the variations of the mean, rms, maximum and minimum pressure coefficients at the critical tap 2 positioned near the windward roof ridge corner (mid-edge) with wind angle of attack for the 15°, 30°, and 45° gable pitched roof respectively. The critical wind angles are 30° and 300° with the -1.92 and -2.34 minimum pressure coefficients for the 15° pitched roof, 15° and 345° with the -1.53 and -1.70 minimum pressure coefficients for the 30° pitched roof, and 0° and 225° with the -1.62 and -1.54 minimum pressure coefficients for the 45° pitched roof. While pressure distribution is almost symmetric for 15° pitched roof, there is no symmetry at the pressure distributions of tap 2 for 30° and 45° pitched roofs.

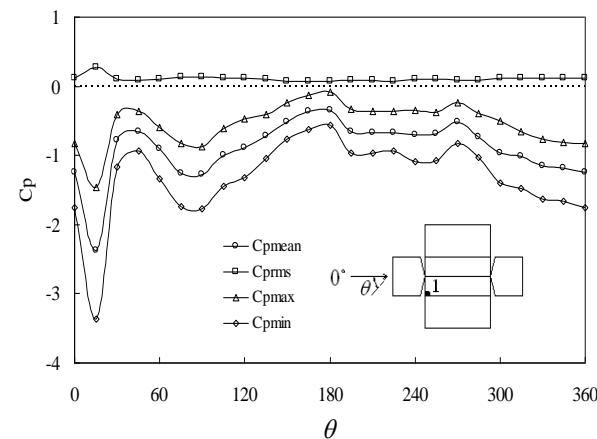


(b)

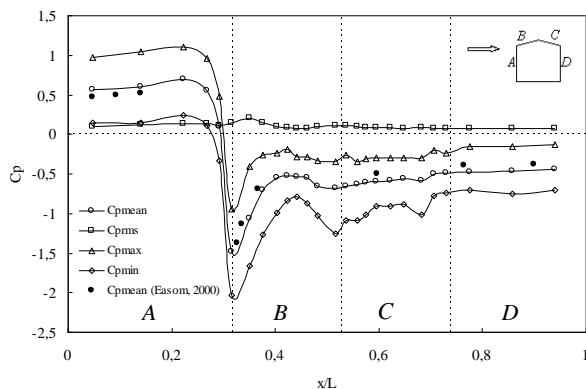


(c)

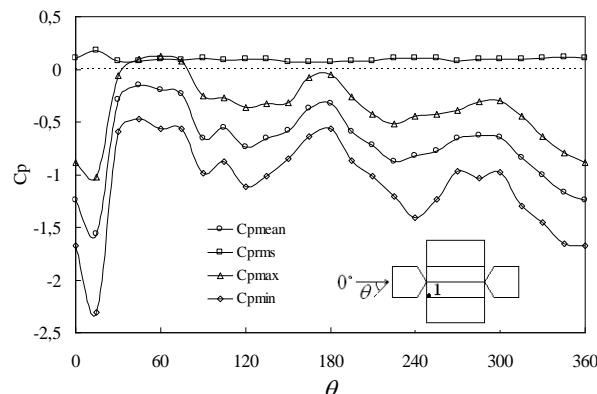
Figure 4. Variation of pressure coefficients along the mid-axis of building models for $\theta=90^\circ$. (a) $\alpha=15^\circ$ (b) $\alpha=30^\circ$ (c) $\alpha=45^\circ$



(a)



(a)



(b)

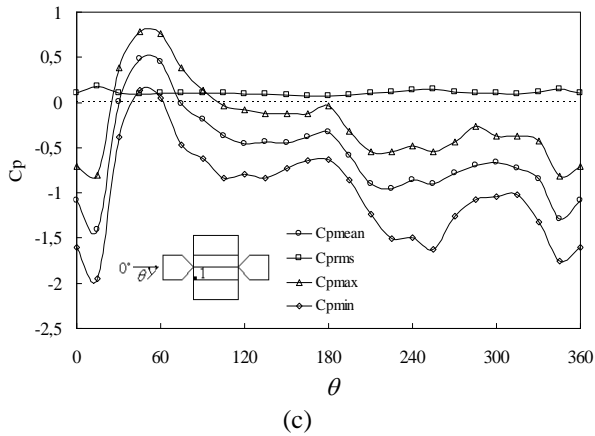


Figure 5. Variation of pressure coefficients with wind direction for tap 1 on the roof corner (a) $\alpha=15^\circ$ (b) $\alpha=30^\circ$ (c) $\alpha=45^\circ$

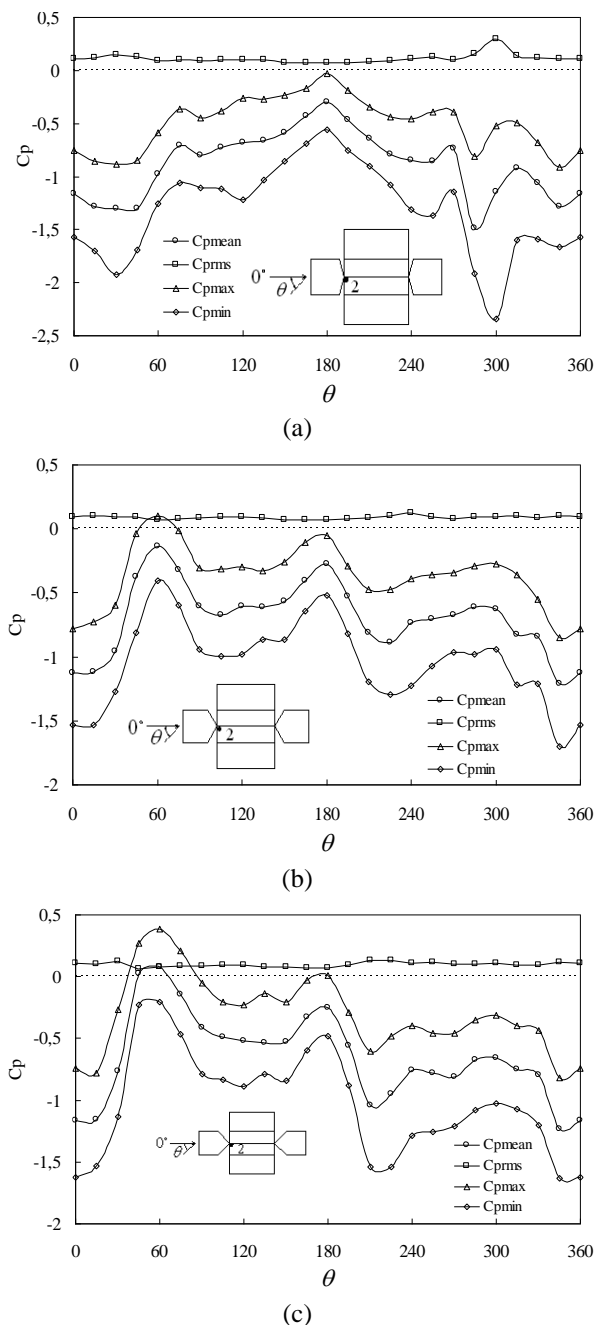


Figure 6. Variation of pressure coefficients with wind direction for tap 2 on the roof ridge corner (a) $\alpha=15^\circ$ (b) $\alpha=30^\circ$ (c) $\alpha=45^\circ$

Figures 7a-e show the contours of mean and minimum pressure coefficients for wind angle 0° on the models with the 15° , 30° , and 45° gable pitched roof respectively. According to the contour plots given in Figures 7a and b for roof pitch of 15° , pressure fields on all surface of the roof are negative. Most critical pressure coefficients occur near the windward roof corner as mean -1.28 and minimum -1.75 . The negative values of mean and minimum pressure coefficients on all measurement points indicate a suction effect on the roof. This effect decreases toward the leeward edge of the roof. Side walls of the model are also under similar effects to that of the roof. Figures 7c and d illustrate pressure contours for roof pitch of 30° . For this roof pitch, the most critical mean and minimum pressure coefficients on the model are obtained near the windward roof corner as -1.24 and -1.71 respectively. Suction that is critical along the gable over the front edge decreases progressively toward the rear edge of the roof. The side walls of the model have also suction effect decreasing from the leading edge to the rear edge. Mean and minimum local pressure distributions for roof pitch of 45° are given in Figures 7e and f. The most critical values on the model are measured as mean -1.25 and minimum -1.68 near the windward roof ridge corner. Concluding from the pressure contours for 0° wind angle, 15° pitched roof is more critical than the others. Figures 8a-e show the contours of mean and minimum pressure coefficients for 45° wind angle on the models with the 15° , 30° , and 45° gable pitched roof respectively. Mean and minimum local pressure distributions for roof pitch of 15° are illustrated in Figures 8a and b. The most critical values on the model are -1.51 as mean and -3.06 as minimum near the windward roof ridge corner. Critical regions for suction are roof edge of the windward side, windward roof corner and the eaves for this oblique angle. Leeward side of the roof is less exposed to the suction effect. As pressure coefficients measured on the windward side wall take positive values on the major part of the surface, leeward side wall takes negative values. This is because of the suction effect on the leeward wall of the building. Figures 8c and d give mean and minimum local pressure contour distributions for the roof pitch of 30° . The most critical mean and minimum pressure coefficients on the model are measured near the leeward roof corner as -1.00 and -1.79 respectively. The most critical regions for suction are roof corner and the roof ridge corner of leeward side. Similar to the 15° roof pitch case, as pressure coefficients measured on the windward side wall take positive values on the major part of the surface, the leeward side wall takes negative values. Mean and minimum local pressure distributions for 45° roof pitch are shown in Figures 8e and f. The most critical mean and minimum pressure coefficients on the model are measured near the leeward roof corner as -0.95 and -1.82 respectively. The values on the leeward part of the roof are more critical than the windward part of the roof. Similar to the 30° roof pitch case, suction effect becomes critical on the leeward roof corner and the

roof ridge corner. The pressure coefficients measured on the windward side wall take positive values on the major part of the surface, whereas the leeward side wall takes negative values. The 45° wind angle is more critical for the suction effects on the roofs when compared with the wind angle of 0° . Figures 9a-e show the contours of mean and minimum pressure coefficients on the models with the 15° , 30° , and 45° gable pitched roof respectively for wind direction of 90° . Measurements for the roof pitch 15° are given in Figures 9a and b. The most critical mean and minimum pressure coefficients on the model are obtained near the windward roof corners as -1.46 and -2.15 respectively. Suction effects along the windward leading edge and the side edge are more critical than the leeward part of the roof surface. Pressure fields on the surface of windward wall are all positive because of pushing effect except the effect of the flow separating from the windward wall edge and weak suction effect at the roof edges. Leeward wall of the building has a weak suction effect compared to the roof surface. Figures 9c and d show mean and minimum local pressure distributions for the roof pitch of 30° . The most critical mean and minimum pressure

coefficients on model are measured near the leeward roof corners as -0.79 and -1.26 respectively. Suction effect on the leeward roof surface is more critical than on the windward roof surface because of its direct exposure to wind. Mean and minimum local pressure distributions for roof pitch of 45° are illustrated in Figures 9e and f. The most critical mean and minimum pressure coefficients on the model are measured near the roof rear ridge corner as -0.95 and -1.82 respectively. Positive pressure fields occur at the windward wall and on the roof of the building because of pushing effect. Negative pressure fields form on the leeward roof and on the rear wall surfaces due to the flow separating from the roof ridge. Leeward wall of the model has a weaker suction effect than the leeward roof surface. Minimum values of fluctuating pressures denoting the magnitude of suction are smaller 30% than the mean values. These minimum values occurring near the roof edge denote high suction. Finally, suction loads on the roofs are more critical for 45° wind direction. Kanda and Maruta (1993) also noted that critical suction values of mean and peak pressures occur at the wind direction of 45° .

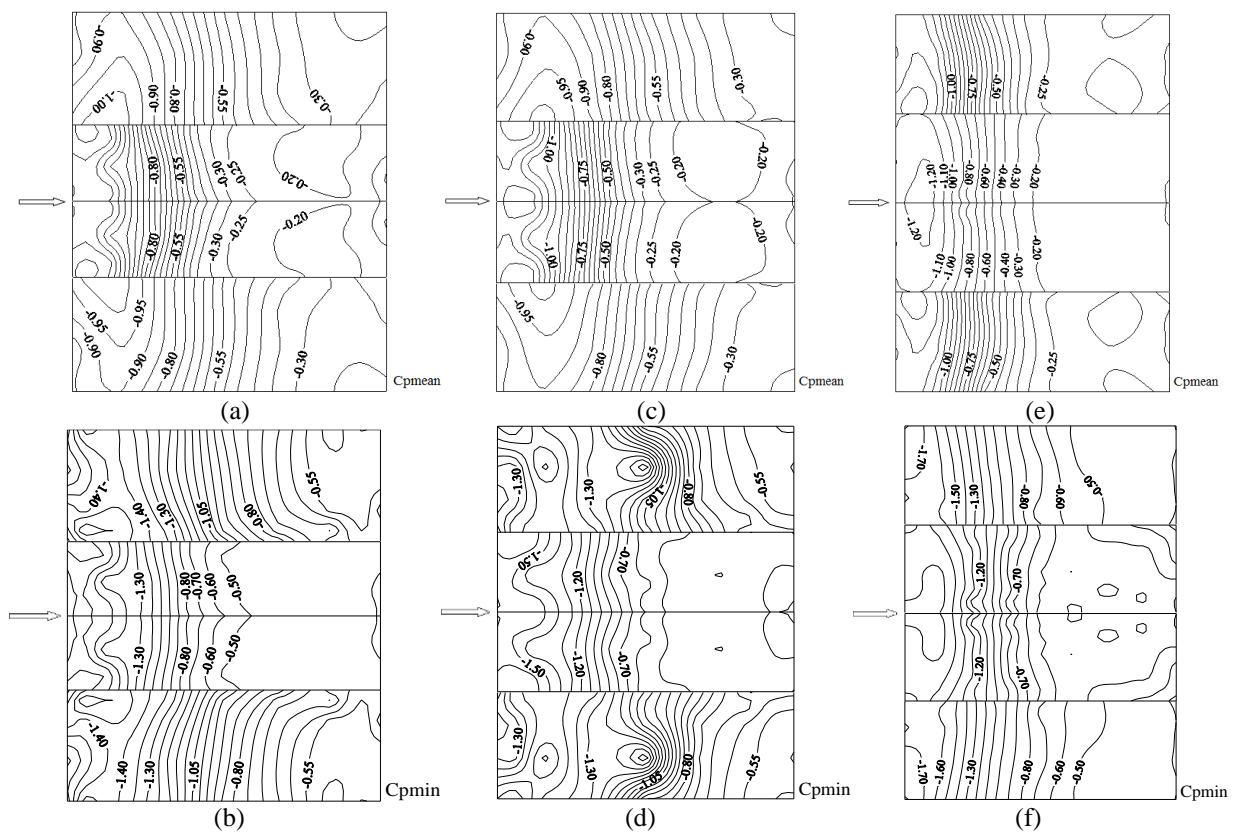


Figure 7. Mean and minimum pressure coefficient contour plots for wind orientation parallel to the roof ridge ($\theta=0^\circ$) (a,b) $\alpha=15^\circ$ (c,d) $\alpha=30^\circ$ (e,f) $\alpha=45^\circ$

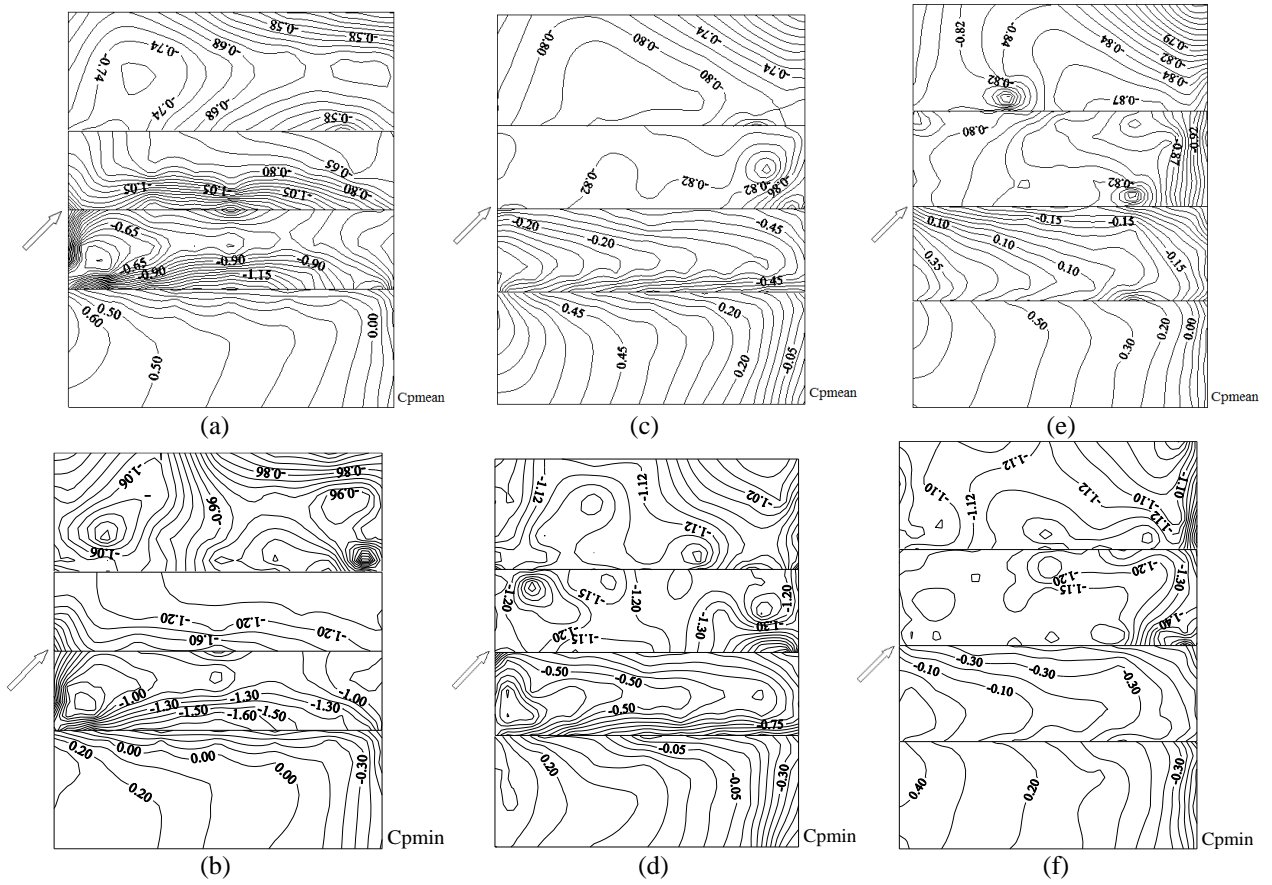


Figure 8. Mean and minimum pressure coefficient contour plots for wind orientation oblique to the roof ridge ($\theta=45^\circ$)
(a,b) $\alpha=15^\circ$ (c,d) $\alpha=30^\circ$ (e,f) $\alpha=45^\circ$

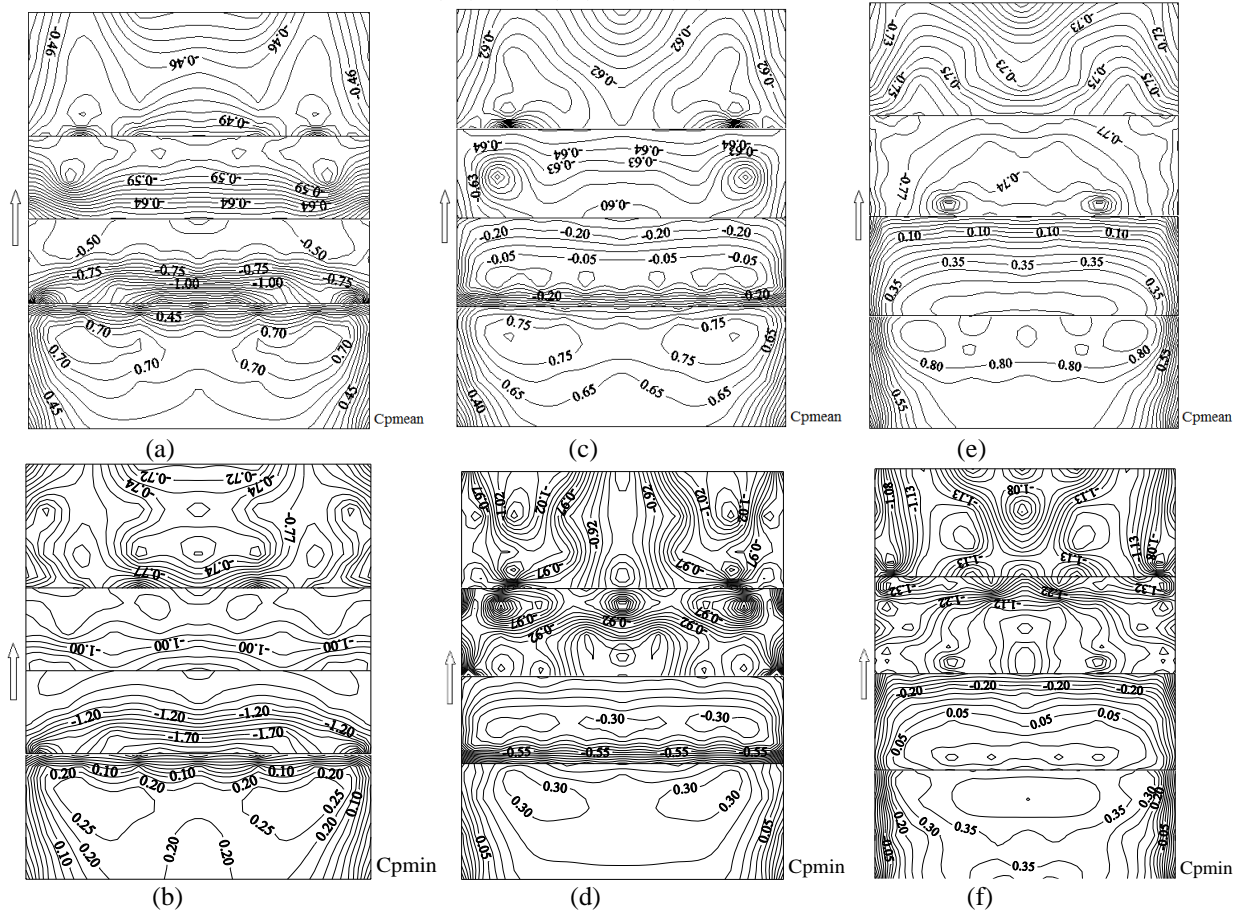


Figure 9. Mean and minimum pressure coefficient contour plots for wind orientation normal to the roof ridge ($\theta=90^\circ$)
(a,b) $\alpha=15^\circ$ (c,d) $\alpha=30^\circ$ (e,f) $\alpha=45^\circ$

Figures 10a-b illustrate the effect of roof pitch on the mean and the minimum pressure coefficients along the mid-axes of building models for wind angle of 90° respectively. Positive pressure distributions occur on the windward walls of the models which are directly exposed to wind due to the pushing effect for all tested roof pitches. For the 15° and 30° roof pitches, pressure coefficients are negative on all the roofs. Pressure coefficients take minimum values near the leading edge of the roofs and then increase maximum values and again decrease on the windward roofs. This behavior is due to the reverse flow region incurred flow separating from the leading edge. Reverse flow regions decrease with increasing roof pitch. Pressure coefficients monotonically decrease on the windward roof for the roof pitch of 45° . No reverse flow region and negative pressure on the windward roof for 45° roof pitch occur. Flow separating from the roof ridge forms similar negative pressure coefficients on the leeward roofs and the rear walls for all tested roof pitches. It is seen that 15° roof pitch produces more critical suction effect than the 30° and 45° roof pitches in case of 90° wind angle. Eaton *et al.* (1975) declared that suction loads increase with decreasing roof pitch and critical suction is effective for a short distance from windward edge. Minimum values of the fluctuating pressures denoting the magnitude of suction effect are 30% more critical than the mean values.

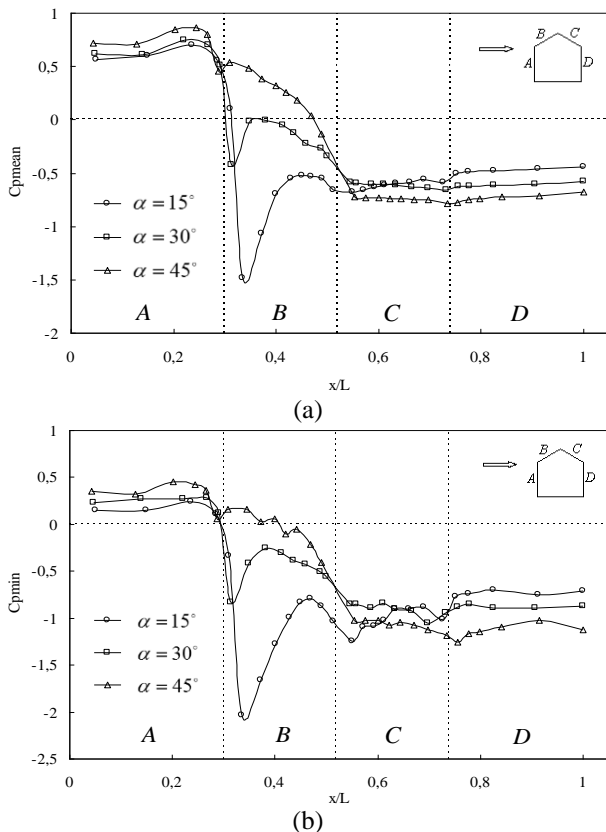


Figure 10. The effect of roof pitch on the pressure coefficient along the mid-axes of building models for $\theta=90^\circ$ (a) C_{pmean} (b) C_{pmin}

The effect of roof pitch on the roof corner pressures is shown in Figures 11a-b as the mean and the minimum pressure coefficient with different wind angle respectively. It is seen that the pressures distributions are

affected from roof pitch in the range of 0° and 150° wind angles. The most critical roof pitch is shown as 15° and critical suction decreases with increasing roof pitch.

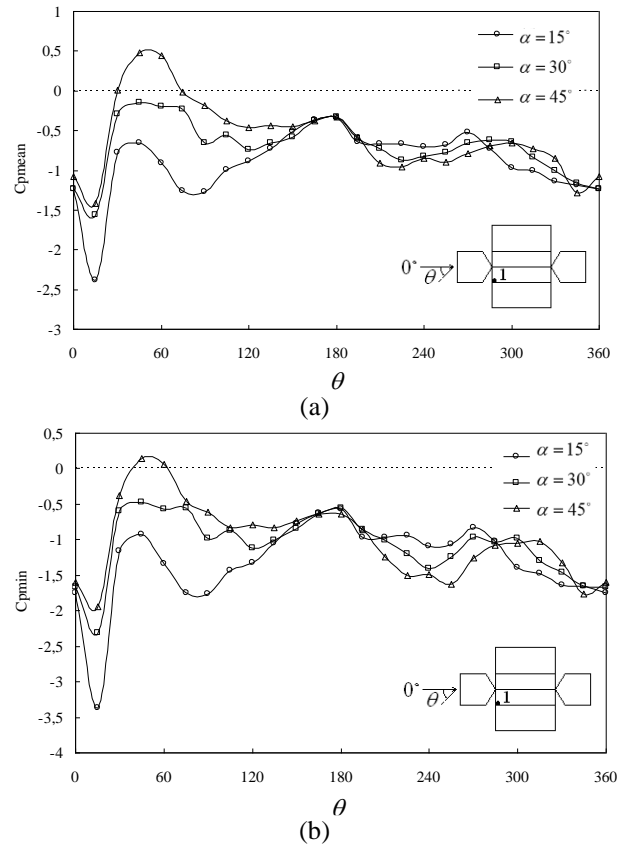
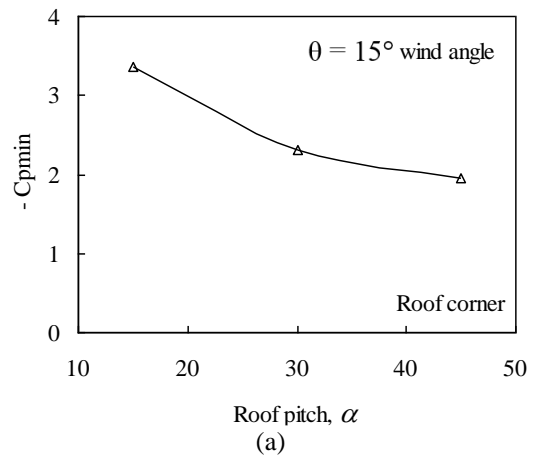


Figure 11. The effect of roof pitch on the pressure coefficient with wind direction for tap 1 on the roof corner (a) C_{pmean} (b) C_{pmin}

Variation of the minimum pressure coefficients on the roof corners and on the roof ridge corners of the gabled roofs are given in Figures 12a and b respectively. For 15° wind angle, the highest suction loads occur on the roof corners and the suction decreases with increasing roof pitch. It is seen that minimum peak pressure on the 45° pitched roof corner is weaker 40% than the minimum peak pressure on the 15° pitched roof corner (Figure 12a). Minimum peak pressures on the roof ridge corners show difference with the wind angle and roof pitch. The critical wind angles are 60° , 15° and 0° for 15° , 30° and 45° pitched roofs respectively (Figure 12b)



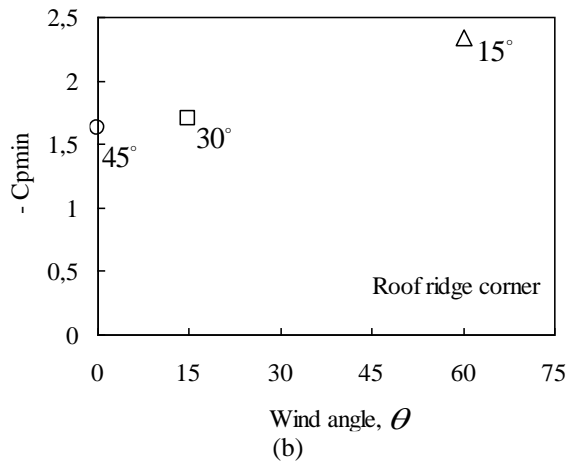
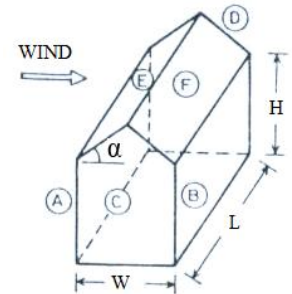


Figure 12. Variation of the minimum pressure coefficient over the gable roofs (a) Roof corner (b) Roof ridge corner

Area-averaged mean pressure coefficients are given for A, B, E and F faces of gabled roof building models with different pitch angles at wind angle of 90° in Table 1. The windward walls facing the flow, A, show positive pressures because of pushing effect and the magnitude of pressure coefficient increases slightly with increasing roof pitch. There are negative pressures on the leeward walls, B, for all the models and the magnitude of suction increases significantly with the increasing roof pitch. Mean pressure coefficients on the roofs are affected from the roof pitch as shown in columns E and F. It is seen that negative pressures on the leeward roof are more critical than those on the windward roof except the roof pitch of 15° . With increasing roof pitch, the magnitude of negative pressure coefficients decreases on the windward roof while it increases on the leeward roof. Only for 45° roof pitch, mean pressure coefficient takes positive value on the windward roof.

Table 1. Area-averaged mean pressure coefficients for gabled roof building models ($\theta = 90^\circ$)

Roof pitch	Area-averaged mean pressure coefficients (C_{pmean})					
	A	B	C	D	E	F
$\alpha = 15^\circ$	0.55	-0.46	-	-	-0.71	-0.59
$\alpha = 30^\circ$	0.60	-0.61	-	-	-0.17	-0.62
$\alpha = 45^\circ$	0.66	-0.73	-	-	0.22	-0.76



CONCLUSION

In this study, wind pressure distributions on the three gable roofed building models of 15° , 30° , and 45° roof pitch have been investigated experimentally to determine the effect of roof pitch on the wind pressure. The mean and fluctuating wind pressures are measured on the building models to reveal the changes in pressure distributions. The results show that the pressure distributions on the roofs are significantly influenced by the roof pitch. Pressure coefficients on the windward walls of building models are positive due to the pushing effect. Negative pressure fields occur both on the roofs and leeward walls of the building models because of flow separated from the leading edges and ridges of the roofs. At the 90° wind angle, for the 15° and 30° roof pitches, pressure coefficients are negative on all the roofs and reverse flow regions occur on the front part of the windward roof. Pressure coefficients monotonically decrease on the windward roof for the roof pitch of 45° and there is no reverse flow region and the negative pressure value on the windward roof for this roof pitch. Flow separating from the roof ridge forms similar negative pressure coefficients on the leeward roofs and rear walls for all tested roof pitches. The 15° roof pitch produces more critical suction effect on the roofs than those of the 30° and 45° roof pitches. The critical wind angle is found as 15° at the windward roof corner for all tested roof pitches. The highest suction loads on the roof corners occur at this wind angle and suction effect decreases with increasing roof pitch. The most critical

minimum pressure coefficient for all of the measurements is -3.36 near the windward roof corner for 15° wind angle. Minimum peak pressure on the 45° pitched roof corner is 40% weaker than that of the 15° pitched roof corner. Pressure contour distributions on the building models with gable roofs show that the most critical wind direction is 45° . Minimum values of fluctuating pressures denoting the magnitude of suction effect are 30% more critical than the mean values.

REFERENCES

- Agui J.H. and Andreopoulos J., 1992, Experimental Investigation of a Three-Dimensional Boundary Layer Flow in the Vicinity of an Upright Wall Mounted Cylinder, *ASME Transactions Journal of Fluids Engineering*, 114, 566-576.
- Banks D., Meroney R.N., Sarkar P.P., Zhao Z. and Wu F., 2000, Flow Visualization of Conical Vortices on Flat Roofs with Simultaneous Surface Pressure Measurement, *Journal of Wind Engineering and Industrial Aerodynamics*, 84, 65-85.
- Barnard R.H. and Driviere J., 1994, Wind Velocities over Pitched Roofs, *Journal of Wind Engineering and Industrial Aerodynamics*, 52, 345-358.
- Case P.C. and Isyumov N., 1998, Wind Loads on Low Buildings with 4:12 Gable Roofs in Open Country and

- Suburban Exposures, *Journal of Wind Engineering and Industrial Aerodynamics*, 77-78, 107-118.
- Davenport A.G. and Surry D.J., 1974, The Pressures on Low Rise Structures in Turbulent Wind, *Canadian Structural Engineering Conference*, Ottawa 1-39.
- Easom G., 2000, Improved Turbulence Models for Computational Wind Engineering, *PhD Thesis*, School of Civil Engineering The University of Nottingham.
- Eaton K.J., Mayne J.R. and Cook N.J., 1975. Wind Loads on Low Rise Buildings Effects of Roof Geometry, *4th International Conference on Wind Effects on Buildings and Structures*, London.
- Gavanski E., Kordi B., Kopp G.A. and Vickery P.J., 2013, Wind Loads on Roof Sheathing of Houses, *J. Wind Eng. Ind. Aerodyn.*, 114, 106-121.
- Ginger J.D. and Letchford C.W., 1992, Peak Wind Loads under Delta Wing Vortices on Canopy Roofs, *Journal of Wind Engineering and Industrial Aerodynamics*, 43, 1739-1750.
- Ginger J.D. and Letchford C.W., 1995, Pressure Factors for Edge Regions on Low Rise Buildings Roofs, *Journal of Wind Engineering and Industrial Aerodynamics*, 54-55, 337-344.
- Ginger J.D., Reardon G.F. and Whitbread B.J., 2000, Wind Load Effects and Equivalent Pressures on Low Rise House Roofs, *Engineering Structures*, 22, 638-646.
- Ginger, J.D. and Holmes, J.D. 2003, Effect of Building Length on Wind Loads on Low Rise Buildings with a Steep Roof Pitch, *Journal of Wind Engineering and Industrial Aerodynamics*, 91, 1377-1400.
- Guirguisa N.M., Abd El-Aziz A.A. and Nassief M.M., 2007, Study of Wind Effects on Different Buildings of Pitched Roofs, *Desalination*, 209, 190-198.
- Holman J.P., 1994, *Experimental Methods for Engineers*, McGraw-Hill Book Company, New York.
- Holmes J.D., 1981, Wind Pressures on Houses with High Pitched Roofs, *Wind Engineering Report 4/81*, Dept. of Civ. & Sys. Eng., James Cook Univ. of North Queensland, Townsville Queensland Australia.
- Hu H., Yang Z., Sarkar P. and Haan F., 2011, Characterization of the Wind Loads and Flow Fields around a Gable-Roof Building Model in Tornado-Like Winds, *Exp. in Fluids*, 51, 835-851.
- John A.D., Singla G., Shukla S. and Dua R., 2011, Interference Effect on Wind Loads on Gable Roof Building, *Procedia Engineering*, 14, 1776-1783.
- Kanda M. and Maruta E., 1993, Characteristics of Fluctuating Wind Pressure on Long Low Rise Buildings with Gable Roofs, *Journal of Wind Engineering and Industrial Aerodynamics*, 50, 173-182.
- Kawai H. and Nishimura G., 1996, Characteristics of Fluctuating Suction and Conical Vortices on a Flat Roof in Oblique Flow, *Journal of Wind Engineering and Industrial Aerodynamics*, 60, 211-225.
- Kumar K.S., 1997, Simulation of Fluctuating Wind Pressures on Low Building Roofs, *PhD Thesis*, Concordia University, Canada.
- Kumar K.S. and Stathopoulos T., 1998, Power Spectra of Wind Pressures on Low Building Roofs, *Journal of Wind Engineering and Industrial Aerodynamics*, 74-76, 665-674.
- Meecham D., Surry D. and Davenport A.G., 1991, The Magnitude and Distribution of Wind Induced Pressures on Hip and Gable Roofs, *Journal of Wind Engineering and Industrial Aerodynamics*, 38, 257-272.
- Oliveira P.J. and Younis B.A., 2000, On the Prediction of Turbulent Flows around Full Scale Buildings, *Journal of Wind Engineering and Industrial Aerodynamics*, 86, 203-220.
- Parmentier B., Hoxey R., Buchlin J.M. and Corieri P., 2002, The Assessment of Full Scale Experimental Methods for Measuring Wind Effects on Low Rise Buildings, *COST Action C14, Impact of Wind and Storm on City Life and Built Environment*, Nantes France.
- Prasad D., Uliate T. and Ahmed M.R., 2009, Wind Loads on Low Rise Building Models with Different Roof Configurations, *International Journal of Fluid Mechanics Research*, 36(3), 231-243.
- Saathoff P.J. and Melbourne W.H., 1989, The Generation of Peak Pressures in Separated/Reattaching Flows, *J. Wind Eng. Ind. Aerodyn.*, 32, 121-134.
- Stathopoulos T., 1984, Wind Loads on Low-Rise Buildings: A Review of the State of the Art, *Engineering Structures*, 21, 629-638.
- Stathopoulos T. and Mohammadian A.R., 1986, Wind Loads on Low Buildings with Mono Sloped Roofs, *Journal of Wind Engineering and Industrial Aerodynamics*, 23, 81-97.
- Zhang Y., Hu H. and Sarkar P.P., 2014, Comparison of Microburst Wind Loads on Low Rise Structures of Various Geometric Shapes, *J. Wind Eng. Ind. Aerodyn.*, 133, 181-190.